# Journal of Materials Chemistry

www.rsc.org/materials

Volume 21 | Number 41 | 7 November 2011 | Pages 16273–16652

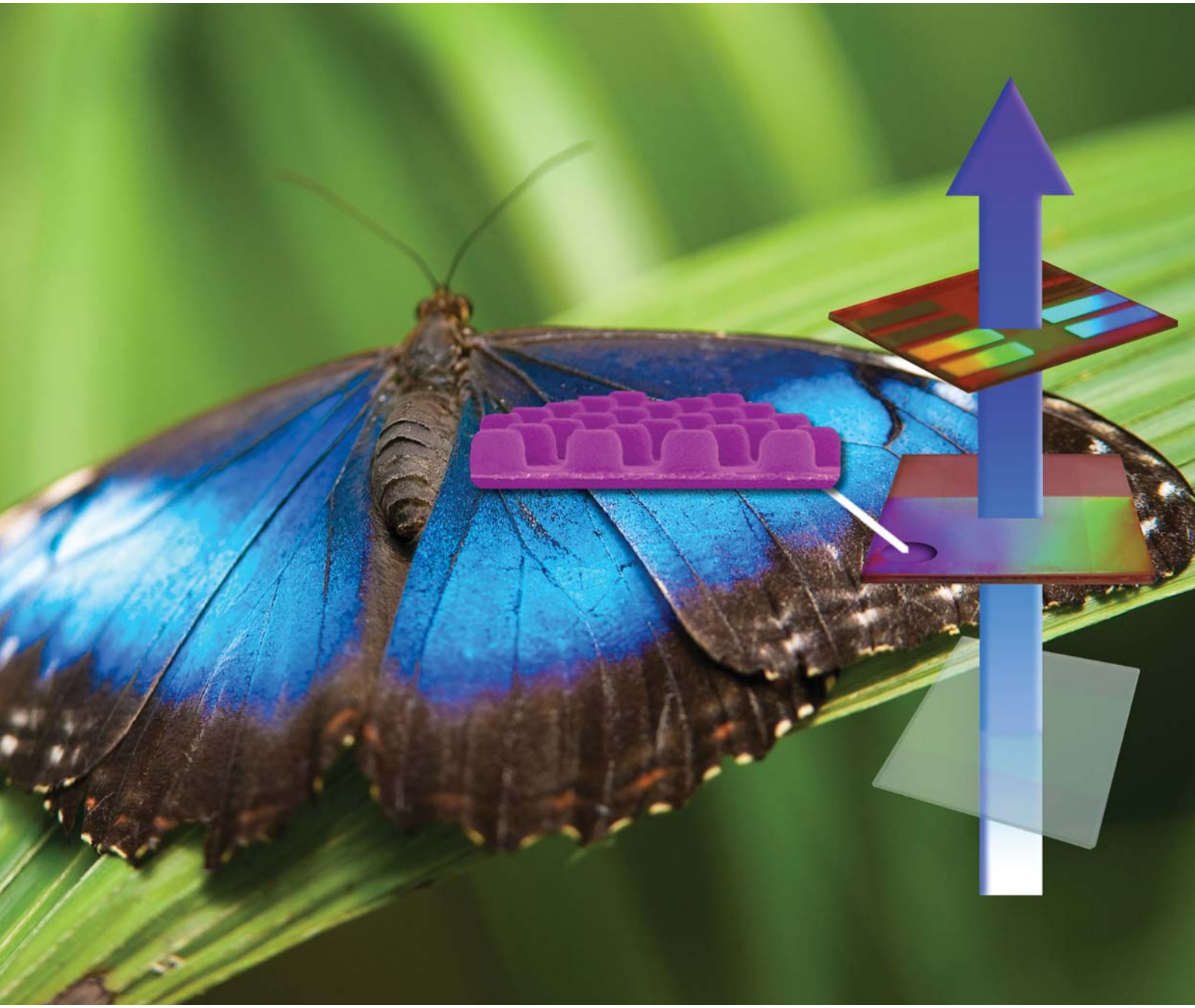

ISSN 0959-9428

RSC Publishing

**FEATURE ARTICLE**
Edward T. Samulski *et al.*
Light-trapping nano-structures in organic photovoltaic cells

International Year of CHEMISTRY 2011

0959-9428(2011)21:41;1-G

Journal of Materials Chemistry

Dynamic Article Links

Cite this: *J. Mater. Chem.*, 2011, **21**, 16293

www.rsc.org/materials

FEATURE ARTICLE

# Light-trapping nano-structures in organic photovoltaic cells

**Doo-Hyun Ko,[a] John R. Tumbleston,[b] Abay Gadisa,[a] Mukti Aryal,[ab] Yingchi Liu,[b] Rene Lopez[b] and Edward T. Samulski*[a]**

***Received 24th May 2011, Accepted 7th July 2011***
**DOI: 10.1039/c1jm12300a**

We review nano-structures used as light trapping schemes in organic photovoltaic (OPV) cells. Light management *via* nano-structures enables one to exploit sub-diffraction limit properties, thereby giving access to enhanced light absorption in OPV cells. Light trapping schemes have been demonstrated in the form of surface plasmons, anti-reflection coatings, and photonic crystal patterns. Versatile methods are now available to facilitate fabrication of such nano-structures on sufficiently large areas for OPV applications.

## 1. Introduction

Organic photovoltaic (OPV) cells are being intensely studied because of their putative advantageous processing features: devices can be printed in a roll-to-roll (R2R) fashion enabling large-scale production at low cost. At the same time, efficiency of OPVs remain under 10%, so any methodology compatible with R2R processing that might enhance performance is of considerable interest. The comparatively high extinction coefficient of organic semiconductors compared to inorganic counterparts can be advantageous. Films of only a few hundred nanometres can achieve complete absorption. However, incommensurate length scales—the absorption length (~100 nm) and exciton diffusion length (~10 nm)—limit the performance of OPV cells and, in turn, their widespread adoption as a renewable energy source. The bulk heterojuction (BHJ)[1,2] morphology, a bicontinuous, nanoscale, phase-separated donor and acceptor components of OPV cells attempts to resolve the intrinsic length-scale mismatch. However, carrier transport through the contorted BHJ morphology remains an obstacle that still imposes thickness limitations on the photoactive layer.[3,4] The BHJ film thickness can be reduced if technologically-viable, robust, cheap light management techniques are employed. Herein we review various light management schemes that have been explored in the context of enhancing OPV device efficiency.

A number of light trapping schemes that fall under the umbrella of ray optics approaches such as collector mirrors,[5] fiber based,[6,7] V-fold[8–10] and micro lenses,[11,12] have been investigated. From a ray-optics perspective, conventional light trapping exploits the effect of total internal reflection by roughening the entrance interface and randomizing the light propagation direction inside the active materials. This results in a much longer interaction distance inside the material and hence a substantial absorption enhancement that is

[a]*Department of Chemistry, University of North Carolina at Chapel Hill, Caudill and Kenan Laboratories CB 3290, Chapel Hill, NC, 27599-3290, USA. E-mail: et@unc.edu; Fax: (+1) 919-962-2388; Tel: (+1) 919-962-15661*

[b]*Department of Physics and Astronomy, University of North Carolina at Chapel Hill, Phillips Hall CB 3255, Chapel Hill, NC, 27599-3255, USA*

**Doo-Hyun Ko**

*Doo-Hyun Ko received his B.S. degree (1996) and M.S. degree (1998) in Chemistry from the Korea University, Korea. He was a research scientist in the LG Display from 1998 to 2005 studying LCDs and OLEDs. He earned his Ph.D. (2010) in Chemistry with Prof. Edward T. Samulski at the University of North Carolina at Chapel Hill researching nano-patterned organic photovoltaics.*

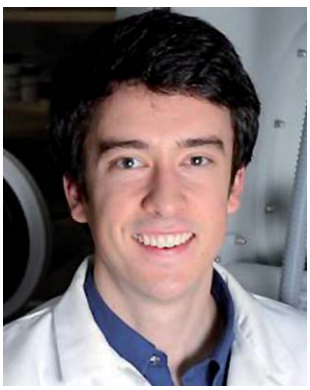

**John R. Tumbleston**

*John R. Tumbleston received his M.S. (2008) and Ph.D. (2011) from the Physics and Astronomy Department at the University of North Carolina at Chapel Hill. While working in the group of Prof. Rene Lopez, he conducted research on photonics and carrier transport of polymer solar cells.*

nonetheless limited to $4n^2$ where $n$ is the refractive index of the photoactive material.[13,14] Among many attempts to bypass this limitation, light trapping schemes comprised of highly ordered and periodic nano-structures have been explored. The optical properties of such nano-structures are designed to manipulate light flow to enhance light absorption in the photoactive layer. Recent theoretical studies[15,16] have shown that absorption enhancement factors with appropriately integrated nano-structures in OPV cells are expected to boost absorption up to $12x4n^2$. In particular, photonic crystal (PC) nano-structures may act as a waveguide or mirror and have been explored to improve light trapping efficiency over a range of wavelengths.[17,18] The PC geometry has been theoretically and experimentally investigated for inorganic silicon based photovoltaics[19–22] and has been incorporated into OPV cells[23,24] as well as dye sensitized solar cells.[25–28]

We will summarize recent progress in light trapping schemes involving nano-structures for OPV cells using both surface plasmon and anti-reflection coatings, and PC nano-structures. Note that the June 2011 issue of the *MRS Bulletin* is devoted to photon management for photovoltaics.[29] Finally, recent progress in advanced techniques used to prepare (conductive) organic nano-patterns for fabricating light trapping structures for OPVs will be summarized.

## 2. Plasmonic OPV cells

Surface plasmons have been introduced to trigger high local absorption in OPVs with optically thin films which enhances optical absorption within the material's absorption window. Since surface plasmons are bound electromagnetic oscillations of electrons at the interface between a metal and a dielectric material, their generation usually demands metal nano-particles implanted on surfaces or imbedded in dielectric media.[30–41] Corrugated metal surfaces, usually the electrodes in devices, are also capable of light scattering as well as triggering surface plasmons.[42] In photoactive materials, surface plasmons typically induce enhanced light trapping *via* two distinct physical mechanisms. The first is to excite propagating surface plasmon polariton (SPP) waves at the interface with the active layer where the large SPP electric field enhances polymer light absorption. Secondly, by exciting highly localized surface plasmons in metallic nano-particles and triggering strong resonant light scattering, absorption can also be increased. This resonance scattering near the plasmonic particles occurs only for certain wavelengths since this phenomenon is limited by the particle morphology. More details can be found in previous reviews.[43–45] Commonly, three types of device configurations are considered for effective generation of surface plasmons in OPV cells: 1)

**Abay Gadisa**

*Abay Gadisa received a Ph.D. in Applied Physics in 2006 from Linköping University, Sweden, followed by a research fellowship at University of Hasselt and IMEC, Belgium, investigating optoelectronic properties of organic materials. He is currently a research scholar at the University of North Carolina at Chapel Hill, USA, studying role of morphology in organic donor/acceptor bulk heterojunction films, charge transport in organic films, and photonic structures for photovoltaic applications.*

**Rene Lopez**

*Prof. Lopez obtained his B.S. from the Monterrey Institute of Technology (Mexico), and his M.S. and Ph.D. from Vanderbilt University. After working at Oak Ridge National Laboratory and Vanderbilt he joined the University of North Carolina at Chapel Hill. He currently heads a group investigating photonic structures for organic photovoltaics, dye sensitized solar cells, surface raman enhancement spectroscopy, and evanescent wave amplification in the Department of Physics and Astronomy.*

**Mukti Aryal**

*Mukti Aryal is currently a post doctoral fellow at UNC, Chapel Hill. He received his Ph.D. with Prof. Hu from the University of Texas at Dallas in 2010. His research interests include cost effective nano-fabrication of master templates of regular and bio-inspired complex shapes, hard and soft molding, nano-confinement induced polymer chain ordering, nano-structured and photonic crystal OPV.*

**Edward T. Samulski**

*Edward T. Samulski is Cary Boshamer Professor, University of North Carolina, Chapel Hill. His Ph.D. (Princeton University) preceded postdoctoral fellowships (Groningen and Austin). A founding editor of Liquid Crystals, he demonstrated the existence of a biaxial nematic liquid crystal and is currently exploring nano-structured substrates for high efficiency solar cells.*

outward excitation on the photoactive layer, 2) excitation of the embedded metal nano-particles in the photoactive layer, 3) excitation due to a corrugated metallic grating. We briefly discuss all three in the following sections.

### 2.1. Outward excitation on the photoactive layer

In outward excitation, metal nano-particles embedded in electrode buffer layers[31,33,46] were employed in devices to trigger surface plasmons that strongly scatter into to the overlaying OPV absorbing films. This approach demands the placement of the organic layer within close proximity to couple the surface plasmons effectively. Recently, J.-L. Wu *et al.*[31] have demonstrated solar cells with gold nano-particles (Au NPs) blended into the anodic buffer layer, poly(3, 4-ethylene dioxythiophene):poly (styrene sulfonate) (PEDOT:PSS), to trigger localized surface plasmon resonances (See Fig. 1). This device configuration seems to render a dual benefit, namely absorption enhancement in the OPV films due to the field enhancement and concomitant localized surface plasmon resonance[46] along with a suggested enhanced exciton dissociation probability through the interactions between the plasmons and the photogenerated excitons. As a result, this particular light trapping scheme has improved the overall device power conversion efficiency by more than 18%. Similarly, vapor-deposited and coalesced plasmon-active Ag islands deposited on top of an indium-tin-oxide (ITO) electrode with an overcoat of PEDOT:PSS, was found to couple surface plasmons to the absorbing organic layer.[30] Solution based assemblies of Ag nano-particles on top of either ITO or PEDOT:PSS has also been used in OPV cells.[35] Those investigations show that the Ag-generated surface plasmon energy is accessible over several tens of nano-metres above the source points, which is consistent with similar observations for small molecule solar cells.[41] The density of the nano-particles should be carefully chosen in order to avoid changes in the paths of electrical transport.

Interestingly, surface plasmons can also be triggered by metal nano-wires (nano-gratings) integrated into OPV cells or OLED electrodes. In their recent reports, M.-G. Kang *et al.*[32] have replaced the common OPV anode electrode ITO with silver (Ag) nano-wires and recorded an overall power conversion efficiency increase of 35%. In such devices, absorption enhancement can selectively address specific spectral regions of interest by appropriately choosing the period of the Ag nano-gratings.

### 2.2. Excitation of the embedded metal nano-particles in photoactive layer

Plasmon energy from metal nano-particles can also be efficiently coupled to organic absorbing layers if the metal nano-particles are embedded inside the organic layer.[35,40] The use of bare particles may result in quenching of excited states and free carriers, so nano-particles are commonly coated with a thin (less than the nano-particle radius) dielectric material.[47] This type of architecture is highly influenced by interparticle spacing and particle diameter as shown in Fig. 2.[47]

This plasmonic effect has been demonstrated for tandem OPVs by using silver nano-particles in ultrathin-organic films.[41] Tandem solar cells have been considered to expand the absorption window of OPVs. One challenge for tandem OPVs is matching absorption for the front and back cells that are made to capture different regions of the solar spectrum. An imbalance in photo-generation yield in the two adjoined cells is difficult to avoid. Since only the smallest photocurrent is drawn out of tandem cells, the resulting efficiency can be limited. Therefore, light management strategies are crucial to boost the photocurrent yield that go beyond simply optimizing the active layer thicknesses. This strategy has been investigated for tandem OPVs where silver nano-particles embedded between two neighboured cells enhanced long-range absorption resulting in increased efficiency.[41]

### 2.3. Excitation *via* corrugated metallic gratings

Substantial increases in light absorption can be achieved by triggering surface plasmons from metallic gratings, which occur at the interface between a metal and the photoactive layer. Corrugated metal electrodes are commonly used in OPV cells and organic light emitting diodes (OLED). For OPVs, light is scattered back into the active layer for re-absorption, while in OLED applications corrugated electrodes are used to boost light outcoupling.[48] For OPVs, corrugated metal electrodes in the form of surface diffraction gratings have been investigated theoretically[49] and experimentally.[42,50–54] In principle, the nano-structures of the photoactive layer could be fabricated by patterning organic photoactive materials[42,52,54] or layering the photoactive film on pre-patterned substrates.[50,51,53,55] A subsequent metal deposition step gives rise to the corrugated metal electrode structure.

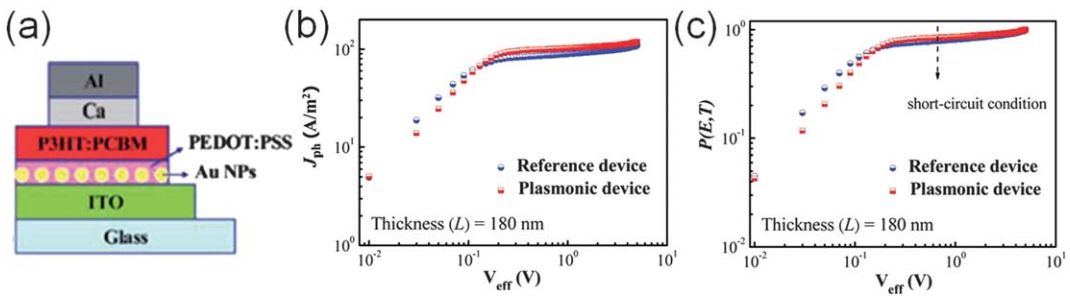


**Fig. 1** (a) Device architecture of OPV devices incorporating Au NPs in the PEDOT:PSS layer. (b) Photocurrent density ($J_{ph}$) plotted with respect to effective bias ($V_{eff}$) for the reference and plasmonic devices, and (c) exciton dissociation probability [$P$(E,T)] plotted with respect to effective bias ($V_{eff}$). The dissociation probabilities for the reference and plasmonic devices under short-circuit conditions were 78.2% and 84.2%, respectively. Figures reproduced with permission from ref. 31, © 2011 ACS.

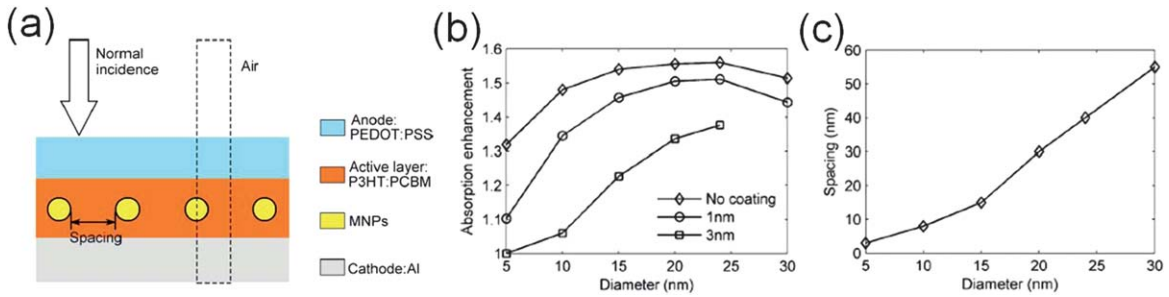


**Fig. 2** (a) Schematic of OPV device architectures with embedded nano-particles. (b) Optimized absorption enhancement as a function of metallic nano-particles (MNP) diameter with and without coating the MNPs with silica. The silica coating helps to avoid quenching of the generated excitons at the MNPs/active layer interfaces. (c) Optimum spacing between neighboring particles corresponding to absorption enhancement in (b). Figures reproduced with permission from ref. 47, © 2009 AIP.

Generation of surface plasmons at an interface between corrugated cathodes and various OPV materials has been demonstrated by K. Tvingstedt *et al.*[42] using a soft lithographical technique to directly pattern the photoactive material. As shown in Fig. 3 (a) and (b), the fingerprint of interface generated plasmons is manifested in the form of a clearly discernible absorption enhancement in the patterned cells compared to the planar cells. S.-I. Na *et al.*[54] systematically studied the light trapping effect of periodic nano-structures for OPV cells in more depth by varying grating amplitudes, dimensions and periodicities. As shown in Fig. 3 (c) and (d), the nano-structures reduce the zeroth order reflected light intensity thereby increasing higher order reflections due to diffraction, which ultimately increases the optical path length in devices. For 2-D OPV gratings, the observed higher $J_{sc}$, 10.9 mA cm$^{-2}$ (reference 9.5 mA cm$^{-2}$) is attributed to the enhanced intensity of diffracted light over the entire absorption spectrum. However, metal electrodes that penetrate into the soft organic films can give rise to losses.[39]

In addition to the enhanced light absorption, a recent study[51] on highly ordered nano-patterned anodes where the photoactive materials were layered on pre-patterned substrates exhibited an additional benefit associated with the increase of the interfacial area between the photoactive layer and the anode, contributing to more effective carrier transport.

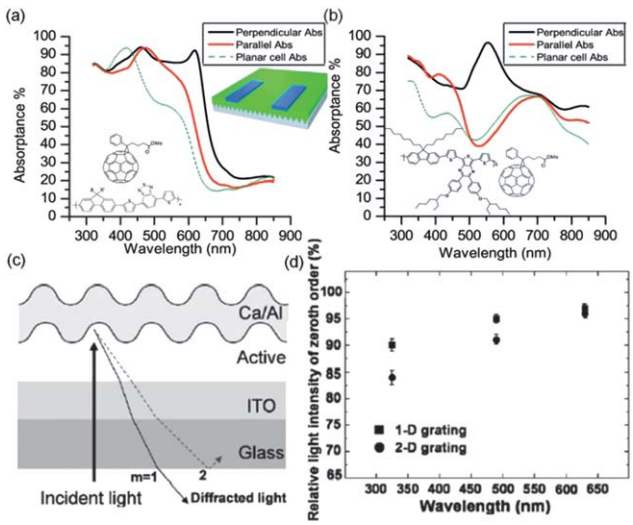


**Fig. 3** (a) Measured absorption ($A = 100 - R$) for APFO3/PCBM on an Al grating and (b) for APFO Green5/PCBM on Ti/Al grating illuminated with different polarizations compared to a planar absorption spectra. A and R stands for absorption and reflectance, respectively. The device structure is shown in the inset. (c) Schematic nano-structured OPV cells with 1D and 2D gratings. The nano-structures prepared by a soft lithographic technique lead to diffraction of the incident light which increases the optical path length in the device. (d) Relative diffraction light intensity of zeroth order for 1D and 2D gratings with 500 nm period and 20 nm depth nano-structures, showing increase of diffracted light for the grating OPV cells compared to the reference. Figures reproduced with permission from: (a) and (b) ref. 42, © 2007 AIP; (c) and (d) ref. 54, © 2008 Wiley.

## 3. Anti-reflection coatings

Nano-structured anti-reflection (AR) coatings are beneficial for silicon solar cells due to the inherent strong reflection from silicon.[56,57] One of the advantages of organic films is their inherent high absorption. However, the various dielectric layers (including the substrate, the photoactive layer, and the buffer layers) included in OPVs trigger a considerable amount of reflection at interfaces leading to optical loses. In order to minimize the losses, various nano-structured AR strategies have been suggested for OPVs including "moth-eye" structures,[58] self-assembled monolayers of nano-silica spheres,[59] 1-D periodically micro-structured lens surfaces,[60] and hierarchically patterned surfaces using template-mediated UV replica molding.[61] For example, self-assembled monolayers of nano-silica spheres induce a broad and red-shifted absorption in P3HT(Poly-(3-hexylthiophene))/PCBM(Phenyl-C61-butyric acid methyl ester) films as a result of reduced reflectance over a wide range of incident angles relative to bare ITO.[59] The additional absorption resulted in increased overall power conversion efficiency at all angles of incidence. Specifically, improvements in power conversion through reductions in reflectance loss increased the performance by nearly a factor of two at the highest angle of incidence (60°) in the presence of an AR nano-structure. This indicates that additional engineering is required to minimize angular-dependent reflection losses. Remarkably, the broadband anti-reflection property leads to improvement of the power conversion efficiency from 1.80% to 2.05% at normal incidence due to the enhanced current density (13.83 mA cm$^{-2}$ from 12.64 mA cm$^{-2}$).[59] Theoretical calculations show that 1-D

 

periodic anti-reflection layers require specific periods for the various angles of incidence.[60] In general, smaller periods are required to reduce the reflection losses at oblique angles.[60]

## 4. Photonic Crystals (PCs)

Photonic crystals (PCs) are defined as dielectric structures with periodic optical properties on the order of the wavelength of light. PCs show a distinct difference from simple diffraction gratings: they are designed to exhibit photonic band gaps where propagation of electromagnetic waves is forbidden, thereby enabling the manipulation of light. Using materials with contrasting optical properties, diffracted light can result in localization[62] and subsequent light trapping over a broad frequency range[63] with the periodicity and the refractive index contrast determining the frequency and magnitude of coupled light. The fascinating ability of PCs to control the flow of light has been exploited to improve performance of optoelectronic devices such as OLEDs,[64–66] sensors,[67–72] and solar cells.[20,27,28,73,74] In this section, PC approaches to enhancing OPV (PC-OPV) cell performance will be discussed.

### 4.1. Bilayer PC-OPV cells

The first investigation of PC-OPV cells were for bilayer devices. D. Duché *et al.*[17] theoretically demonstrated that a PC nanostructured P3HT/PCBM bilayer device could enhance absorption of incident light near the material's band edge ($\lambda > 600$ nm) through Bloch mode coupling. A PC structure consisting of nano-patterned P3HT cylinders (150 nm high, 400 nm diameter and a 500 nm periodicity) embedded in a PCBM layer yields a 35.6% absorption enhancement in the 600 to 700 nm wavelength region relative to a BHJ P3HT:PCBM reference cell. In spite of this absorption enhancement, however, the short exciton diffusion length in P3HT (~10 nm)[4] is expected to hamper the electrical performance of such devices, leading to investigations of alternative designs for PC-OPV cells.

### 4.2. Bulk heterojunction PC-OPV cells

A primary limitation of the bilayer PC-OPV cell architecture is the missmatch in length scales that exists between the PC nanopattern (~500 nm) and the intrinsic distance excitons are able to diffuse prior to recombination (~10 nm). Furthermore, the refractive index difference between electron donors like P3HT and electron acceptors like PCBM is very modest.[75,76] In order to circumvent these two limitations, bulk heterojunction PC-OPV cells have been explored.

Fig. 4 shows representative schematics, a photograph, and cross sectional SEM (scanning electron microscope) images of PC and planar (non-patterned) cells fabricated on the same device substrate. In contrast with the bilayer PC architecture, the BHJ morphology of phase-seprated donor and acceptor components can be nano-patterned (a hexagonal array of posts 180 nm high and a 400 nm periodicity). The nano-patterned P3HT:PCBM BHJ has a relatively high refractive index (~2.1 at 550 nm) that must be back-filled with a comparitavely low refractive index electron transporting material to generate sufficient refractive index constrast, *e.g.*, with nano-crystalline zinc oxide (*nc*-ZnO; ~1.5 at 550 nm). This system has been optically modeled and shown to give absorption enhancements of around 15%.[18] Furthermore, absorption enhancements were demonstrated to scale with the refractive index contrast between the BHJ (P3HT:PCBM) and the electron transporting material (*e.g. nc*-ZnO).[77]

Along with the refractive index contrast, the physical dimensions of PC cell architecture greatly influenced the absorption. For example, the thickness of the BHJ flash layer—the interconnecting BHJ layer between the nano-patterned posts (Fig. 4 (a))—can affect the total absorption. Fig. 5 (a) shows that the absorption is maximized for a flash layer thickness of 40 nm. These comparisons are made by keeping the volume of P3HT:PCBM constant, *e.g.*, thinner flash layers have taller posts, while thicker flash layers have shorter nano-pattern features. Another critical design parameter that influences light absorption in both PC and planar cells is the thickness of *nc*-ZnO, the back-filled refractive index contrast material. For the planar cell, this material is the same as an optical spacer with thickness $d_1$ (Fig. 4 (a)), and for the PC cell, it is the *nc*-ZnO thickness between the top of the BHJ posts and aluminum cathode ($d_3$ in Fig. 4 (a)). Due to variations in optical interference for both cell types as $d_1$ and $d_3$ were changed, factors of two in the absorption were realized (Fig. 5 (b)). Such observations were predicted in optical modeling.[77] Despite these challenges, absorption enhancements of 13% are realized for PC cells when PC and planar cell parameters are separately optimized.[24]

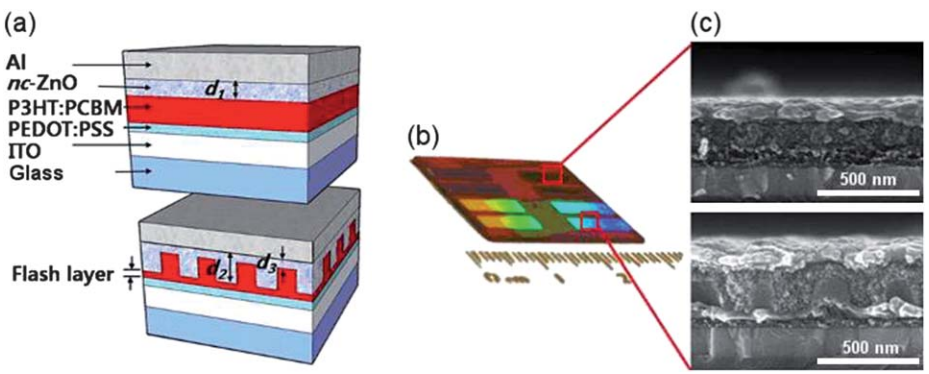


**Fig. 4** (a) Schematic, (b) photograph, and (c) SEM cross sectional images of PC BHJ (bottom) and planar, non-patterned cells (top). As shown in (b), both cell types are fabricated on the same device substrate. Figures reproduced with permission from ref. 24, © 2011 ACS.

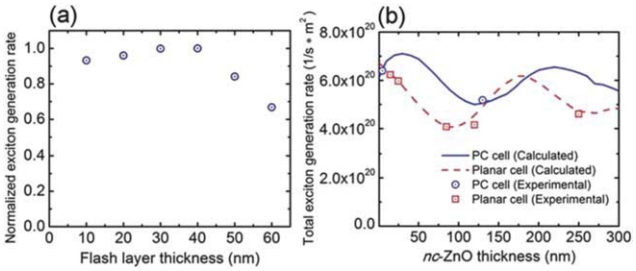


**Fig. 5** (a) The normalized exciton generation rate for a fixed *nc*-ZnO thickness ($d_3 = 20$ nm) is a strong function of the flash layer thickness. (b) Total exciton generation rate as a function of *nc*-ZnO overlayer thickness ($d_3$) and planar film thickness ($d_1$) for PC and planar cells, respectively. Symbols correspond to fabricated devices that lie along the calculated curve as a function of *nc*-ZnO thicknesses. Figures reproduced with permission from ref. 24, © 2011 ACS.

The results of Fig. 5 (b) are from a combination of optical measurements and simulations. Only absorption by the BHJ leads to the creation of excitons that generate a photocurrent. Nevertheless, other device components including the multilayer electrodes are lossy materials. In order to separate these absorption losses, reflection from PC and planar cells were measured and compared to an optical model.[18,77] Using the measured optical properties of all of the device materials, and by varying the physical dimensions around those obtained from SEM, good agreement is achieved between measurement and simulation (Fig. 6 (a)) for the same cells in Fig. 4 with a different BHJ donor, TDPTD (Thermally deprotectable poly thiophene derivatives).[23] Not only does this result validate the optical model, but it also shows the redistribution of optical energy in both PC and planar cells (Fig. 6 (b), (c)).

The measurement of specular reflection also confirms the presence of resonant modes in PC solar cells. Fig. 7 shows measured device reflection and incident photon to current

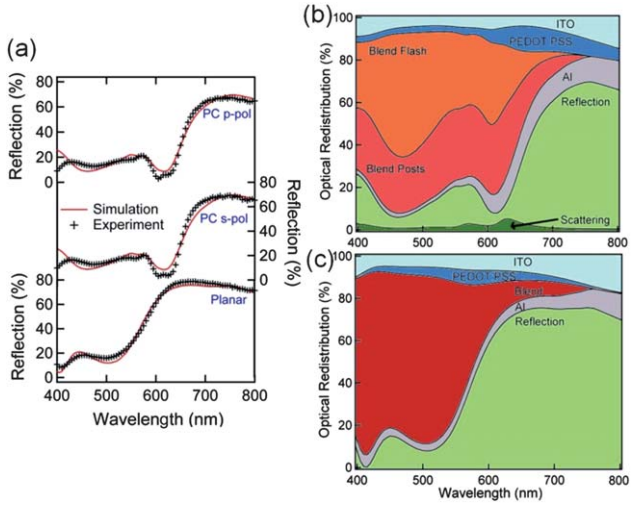


**Fig. 6** (a) Experimental and simulated normal incidence reflection from PC and planar devices. Optical redistribution of (b) PC and (c) planar cells showing the various optical losses in both cell types. Absorption in the blend is the only loss that contributes to photocurrent generation. Figures reproduced with permission from ref. 23, © 2009 ACS.

efficiency (IPCE) as a function of incident angle and polarization for PC cells. Many of the modes red-shift as the incident angle is increased where mode degeneracy is broken (compare number of modes to normal incidence measurements of Fig. 6(a)). The excitation of resonant modes is a critical feature of PC cells as those contribute to absorption enhancements, especially when modes close to the band edge of the photoactive material where the blend absorbs weakly are selectively excited. Absorption enhancements target this region because most BHJ blends, including P3HT:PCBM, absorb very strongly near their absorption maxima. Unlike other light trapping schemes that do not involve nano-structures, targeting specific spectral ranges is at the heart of nano-patterning techniques such as PC-OPV cells.

For both P3HT:PCBM[24] and TDPTD:PCBM[23] solar cells, enhancements in absorption were noted in optical measurements and modeling. In both of these BHJ mixtures, an increase in $J_{sc}$ followed the enhancements predicted by the optical model for the maximally absorbing planar and PC cells when the nc-ZnO thickness was optimized. Along with these devices, other BHJ PC configurations have been explored including inverted OPV cells where the electron transporting layer is nano-patterned instead of the active material.[24] After such nano-patterning, the BHJ is spincoated to fill the nano-structure in the same way as the nc-ZnO was used in the PC cells described above. Furthermore, due to the importance of flash layer thickness on device performance, tandem cells with CuPC (copper phthalocyanine) between the anode and BHJ flash layer have been explored.[24] Even in these cases, the presence of resonant mode excitation has been observed in device reflection.

### 4.3. Reflector PC-OPV cells

Another possible PC application for OPVs is to adapt the PC slab to serve as a reflector in a device where the PC enables a lengthening of the optical path length without a further increase in the photoactive layer. M. Agrawal *et al.*[78] reported light trapping in OPV cells having a high-reflectivity, distributed Bragg mirror where the alternating dielectric layers of $TiO_2$ and $SiO_2$, namely, a 1-D photonic structure, are stacked between the

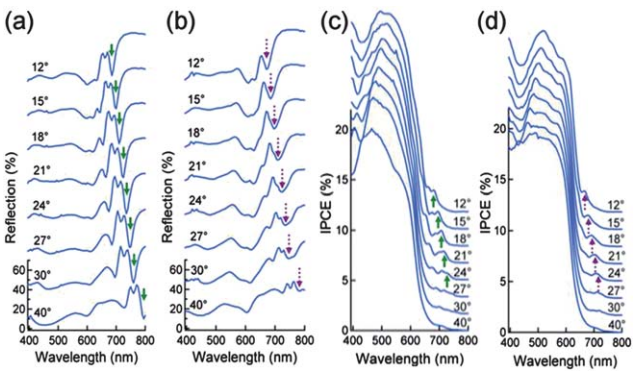


**Fig. 7** Angular dependent zeroth order reflection and IPCE for PC cells with TDPTD:PCBM as the photoactive material for (a) p-polarized reflection, (b) s-polarized reflection, (c) p-polarized IPCE, and (d) s-polarized IPCE. The arrows denote sharp drops in reflection and corresponding increases in IPCE associated with resonant mode excitation. Figures reproduced with permission from ref. 23, © 2009 ACS.

 

ITO and the substrate as shown in Fig. 8 (a). Such OPV cells have the additional advantage of an AR coating as well as an efficient reflector, thereby showing a 40% increase in the short-circuit current. Recently, B. Park *et al.*[79] reported a 2-D PC reflector for OPV cells wherein a hexagonal array of $SiO_2$ nano-rods are embedded in a $SiN_x$ layer as shown in Fig. 8 (b). The PC mirror traps the incident light leading to an absorption enhancement exhibiting a 25% efficiency boost for the BHJ-OPV cell based on P3HT:PCBM. Although the fabrication processes for upscaling of such a PC slab still remains challenging, this approach is promising as it allows for the preparation of the PC structure prior to the photoactive layer deposition, *e.g.*, this could be done with lithography and thereby minimize degradation of the photoactive material during device fabrication.

## 5. Nano-patterning techniques for organic conductive materials for light trapping schemes

The availability of large-area nano-fabrication processes is a key to the commercial adoption of light trapping in OPV cells. Additionally, large-area designed nano-structuring of organic photoactive materials has been posited as a solution to the problem of electron-hole recombination and poor light absorption.[4] Although photolithography has been used for mass production of large-scale optoelectronic devices, the associated UV radiation leads to degradation of conjugated organic materials.[80] Hence, novel nano-patterning methods are needed for nano-structuring organic materials. Moreover, various potential light trapping schemes for OPVs[17,23,24,76] demand new methods to form versatile and scalable patterning of organic materials in OPV cells. The resulting organic photoconductive nano-patterns are also required to be ordered in two or three-dimensions with a length scale comparable to visible light to achieve precise light control.

In the following sections we review hard and soft nanoimprint lithography (NIL). A representative lithographic fabrication strategy for nano-structured OPV cells, including the PC geometry, is shown in Fig. 9.[81] The master templates with desired nano-structures is initially fabricated from a hard material, *e.g.* Si, and either directly used to pattern the conductive organic material *via* hard nanoimprint lithography (Hard NIL) or used to prepare soft replicas from PDMS (poly-dimethylsiloxane) or PFPE (perfluoropolyether)[82,83] that are employed to generate

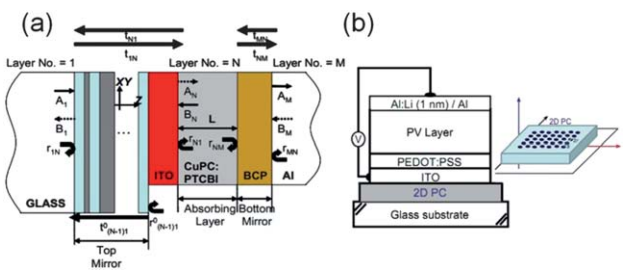


**Fig. 8** Schematics of light trapping OPV cells with (a) a 1-D and (b) a 2-D PC slab placed between ITO and substrate. The PC structure can be tuned for resonant coupling to improve absorption efficiency in photoactive layer. Figures reproduced with permission from: (a) ref. 78, © 2008 OSA; (b) ref. 79, © 2011 Elsevier.

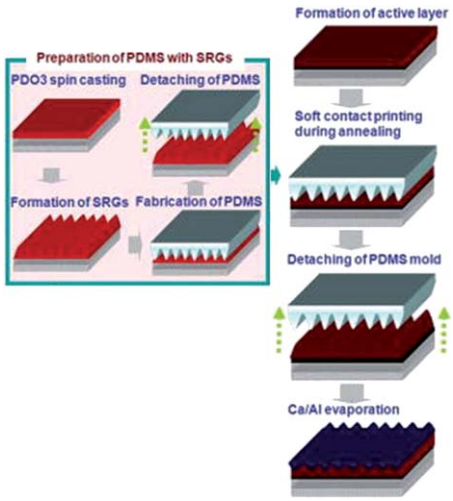


**Fig. 9** Schematic of organic nano-patterning process using soft lithography technique. Figures reproduced with permission from ref. 81, © 2007 AIP.

organic conductive nano-patterns *via* soft nanolithography (Soft NIL). Alternative nano-patterning methods such as direct writing methods using scanning probes and electron beams, and self-assembled block copolymer templates will be briefly introduced to illustrate the growing number of options for nano-patterning OPV cells.

### 5.1. Hard nanoimprint lithography (Hard NIL)

NIL has often been utilized to fabricate large-area nano-structures for OPVs.[84–95] Hard NIL refers to a hot embossing process to transfer the pattern from a rigid mold (generally quartz or Si) to polymer film with the application of heat and pressure. This requires the fabrication of a hard mold with negatively engraved patterns. Among many mold fabrication methods for ordered nano-structures, the most common and cost effective approach employs anodized aluminum oxide (AAO) master templates[96–98] with a hexagonal arrangement of pores; the pore diameter can be easily controlled in the range of 10 nm to 10 μm.[99,100] Fabrication of P3HT nano-structures may be accomplished by infiltration of the AAO pores by solvent assisted wetting and annealing.[91–93,95] However, there are several drawbacks of the AAO molds: they are deformable and present rough surfaces which render them incompatible with NIL. As a result hard Si molds can be prepared by transferring the AAO nano-pore patterns into a Si substrate to fabricate OPV cells using Hard NIL.[94] Confining polymer in nano-structures by means of NIL or other infiltrating methods has resulted in ordering/alignment of polymer chains that can lead to enhanced hole mobility.[84,91–93,95,101] In practice, OPV devices are fabricated by either patterning the P3HT/PCBM blend or infiltrating PCBM into nano-patterned P3HT posts/gratings.[84–86,94,102] Although some improvements in OPV performance was reported due to enhanced hole mobility and increased interface area, the relatively large dimensions of imprinted nano-structures (relative to the exciton diffusion length) limits the IPCE in these devices.[23,24,42,52,54,81,85,86,103] But resolving the length-scale differences is fraught with difficulty: Decreasing feature diameters and spacing effectively limits

feature heights, otherwise feature collapse may occur.[104] Extreme aspect ratios for P3HT features (25 nm diameter rods and 80 nm height) have been reported using Hard NIL.[86]

### 5.2. Soft nanoimprint lithography (Soft NIL)

Rigid materials, such as quartz, glass and silicon used for Hard NIL are inflexible and trapped air prevents conformal and faithful replication of the molded substrate. Furthermore, hard molds require extra surface modification steps (*e.g.*, fluorination) to lower the surface energy and facilitate release.[105] Soft nanoimprint lithography (Soft NIL) obviates these limitations. For this technique, nano-structures are first patterned in a hard master template and then transferred to PDMS[54,81,106–108] or PFPE[23,24,82] soft molds. Those soft (typically gas-permeable) molds are then used to fabricate nano-structures in OPV cell components. Fig. 9 shows a process wherein a hard master template was initially prepared in PDO3 (polydisperse orange 3) by utilizing an interference pattern generated with an $Ar^+$ laser.[109,110] PDMS molds were replicated from the PDO3 master using an elastomeric pre-polymer and curing agent. Patterned nano-features in BHJ solar cells are then fabricated by contacting the PDMS mold with the active layer at elevated temperature. Cathode layer deposition on the patterned surface completes the fabrication process.[54,81] The use of soft, elastomeric materials, such as PDMS, is attractive as it is UV-transparent and has a very low Young's modulus which allows conformal mold contact, even over surface irregularities, without the risk of cracking or breaking.[54,111] Furthermore, mold flexibility facilitates release from the master and allows for multiple molding steps without degradation of the pattern. While PDMS offers some advantages, there are a number of properties inherent to PDMS which severely limit its utility in soft lithography *e.g.* PDMS swells in organic solvents and its surface energy may not be sufficiently low for some applications.[112,113]

Recently, an alternative fluorinated elastomer, PFPE, has been used to overcome some of the shortcoming of PDMS.[82,83,114] PFPE-based materials are liquids at room temperature and can be photochemically cross-linked to yield solvent resistant, chemically robust, durable, elastomers with a tunable modulus. Pattern Replication In Non-wetting Templates (PRINT®) by PFPE has been used to emboss the photoactive layer of PC-OPV cells.[23,24] PRINT is a top-down fabrication method that addresses many of the fundamental shortcomings of other nano-fabrication processes (*e.g.*, precise control of size, shape, and composition). PFPE is a high fidelity molding material that allows for unprecedented ease of release from both the silicon master as well as from patterned replicas without the need for complex surface functionalization. This makes it a good material to use in the routine fabrication of nanometre-scale structures and devices.[114]

### 5.3. Direct nano-pattering by scanning probe and e-beam lithography

Another potential approach for fabricating organic conductive nano-patterns is directly writing the desired features. Direct writing techniques require neither sacrificial photoresist nor photomasks. It yields isolated nano-features in a designated region of the substrate that assume a large variety of shapes like dots, lines and complex figures on a nanometre scale. Direct nano-patterning has been demonstrated with scanning probe lithography (SPL) and e-beam lithography.

Attempts to nano-pattern organic conductive materials *via* SPL have been extensively explored in the form of scanning near-field optical nanolithography,[115–119] electrochemical oxidative nanolithography,[120] thermo chemical nanolithography,[121] and dip pen nanolithography.[122–125] While the probe scans along an organic film in SPL, it can operate in multiple ways: as a heating source for thermochemical nanolithography, a localized strong electric field for electrochemical oxidative nanolithography, and as a UV illumination source for scanning near-field optical lithography. In the case of nano-patterning *via* scanning near-field optical lithography,[119] thin films of PPV (poly(*p*-phenylene vinylene)) precursors were spincoated on a substrate and subsequently illuminated with UV light *via* aperture fiber probes while scanning the film. The non-exposed area was then washed away with methanol and following a thermal conversion of the remaining layer gave rise to PPV nano-pillars (diameter 200 nm with 333 nm pitch), a two-dimensional PC PPV slab.[119]

Dip pen nanolithography has also been introduced as an SPL nano-fabrication technique, where the scanning probe was used to 'print' organic materials on the desired region of a substrate.[122,123] The dip pen nanolithography technique was also applied to control nanoscale phase separation in organic conductive films (see Fig. 10 (a)).[123] A functional alkylthiol was printed on a gold substrate with an atomic force microscope (AFM) tip followed by spincasting a polymer blend solution of P3HT and polystyrene (PS) on the gold substrate. The pre-patterned ink allowed phase-separation during solvent evaporation that resulted in nano-structured films. As shown in Fig. 10 (b), this technique was further exploited to successively facilitate phase-separation from organic photoactive polymer:PCBM blend, and thereby generate organic nano-patterns of MDMO-PPV (poly[2-methoxy-5-(3',7'-dimethyloctyloxy-1,4-phenylenevinylene]) embedded in the PCBM film.[124]

Electron beam lithography, developed from scanning electron microscopes, is another specialized technique for directly

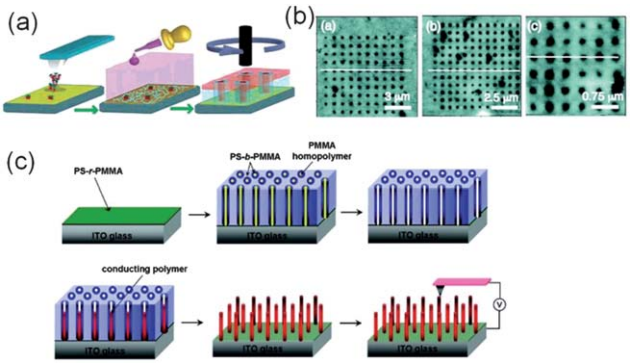


**Fig. 10** Schematic of fabrication routes to organic conductive nano-patterns *via* (a) dip pen nanolithography and (c) block copolymer template. (b) The AFM images demonstrated various periods of patterns of MDMO-PPV (200 nm diameter) embedded in PCBM film prepared from (a). Figures reproduced with permission from: (a) ref. 123, © 2005 ACS; (b) ref. 124, © 2008 ACS; (c) ref. 130, © 2008 ACS.

 

creating extremely fine patterns. While the electron beam scans across a film surface that is sensitive to electron impact, the exposed or non-exposed region of the film is selectively removed. Significant progress has been realized in patterning organic conductive polymers by electron beam lithography.[80,126,127] For instance, Y. Doi *et al.*[80] employed the technique to directly pattern an organic conductive polymer, a polyfluorene derivative, having feature linewidths between 250 nm and 70 nm.[80] The resulting nano-patterned MEH-PPV (Poly[2-methoxy-5-(2-ethylhexyloxy)-1,4-phenylenevinylene]) acted as a highly polarized organic-based distributed feedback laser.[127]

*Via* these direct writing techniques, various organic conductive nano-patterns have been fabricated in materials such as PPV,[115–117,119] MEH-PPV,[127] MDMO-PPV,[124] polyfluorene derivatives,[117,118,124] pentacene,[120] SPAN (sulfonated polyaniline),[122] polypyrrole,[122] P3HT,[123,124] P3OT (poly(3-octylthiophene)),[126] and PEDOT.[128] The nano-pattern resolution was mainly limited by the properties of the scanning probe, including scanning rate, probe geometry, and contact pressure, which yielded nano-patterns ranging from a few nanometres to microns. Even though these can be time consuming processes when large area patterns are desired,[129] they do allow for flexibility in terms of versatile nano-pattern shapes and ranges of materials advantageous to light trapping schemes. Even so, large area nano-patterns and adequately elevated nano-pattern thickness still demand further process optimization for application to light trapping architectures.

### 5.4. Block copolymer templates

The use of selectively etched block copolymers as a template to fabricate nano-patterns has drawn attention because of their intrinsic ability to self-assemble into large two-[130] or three-[131,132] dimensionally ordered structures *via* phase separation. The morphology of block copolymers can be tuned by the block length of copolymers, from nano- to micron scales, which after selective etching of one nano-phase component, leads to their applicability as templating masks. As shown in Fig. 10 (c),[130] PMMA(poly-(methyl metharcylate)) homopolymer and block copolymer (PS-*b*-PMMA) forms a 2-D self-assembled layer on the random copolymer (PS-r-PMMA)/ITO substrate. Subsequently, the template was prepared by selective extracting out the PMMA homopolymer with acetic acid. Starting from the base of the resulting nano-holes in the block copolymer template, conductive nano-rod arrays of polypyrrole[130] or polyaniline[133] have been grown.

## 6. Conclusions

We have reviewed several light trapping schemes which appear to be promising strategies for increasing the performance of OPV cells. Although theoretical calculations suggest that considerable efficiency increases accrue from light absorption enhancement in nano-structured devices, the best reported efficiency with these schemes still remains lower than the highest efficiency reported for conventional organic photovoltaic cells (approaching 8%).[134] Therefore, further work using inherently high efficiency photovoltaic materials is necessary to validate the conjecture that light trapping schemes in OPV cells lead to tangible improvements. In particular, one must overcome potential deleterious effects resulting from the processing used to make nano-structured OPV cells, *e.g.*, additional annealing, residual mold contaminants, chemical cleaning, surface modification *etc.* In particular, the potential changes in the BHJ morphology caused by annealing the nano-confined phase-separated components should be considered in conjunction with carrier mobility changes. Also, the associated cost increase for the nano-patterning process must eventually be factored in. Irrespective of those deterrents the potential advantages from light trapping nano-patterns in OPV cells remain a strong motivation for continued exploration of the subject. The photonic effects reviewed here promise the possibility of using thinner layers of the photoactive material which in turn, has the potential advantage of decreasing the electrical losses in devices leading to an increase in OPV cell performance. Tunable electric field configurations are another by-product of nano-structuring electrodes, one that may impact the extraction efficiency of the photogenerated charge carriers. Additionally, photonic crystal patterning in OPV cells offers the possibility of matching the resonant modes to the absorption spectrum of the photoactive materials thereby enhancing the spectral response of OPV cells.

## Acknowledgements

Support for this work is from NSF (Solar: DMR-0934433) and D.H.K. thanks the UNC-Chapel Hill Institute for the Environment (Carolina Energy Fellows Program). The American Chemical Society Petroleum Research Fund (No.49187-DNI10) also partially supported this research.

## References

1 J. J. M. Halls, C. A. Walsh, N. C. Greenham, E. A. Marseglia, R. H. Friend, S. C. Moratti and A. B. Holmes, *Nature*, 1995, **376**, 498–500.
2 G. Yu, J. Gao, J. C. Hummelen, F. Wudl and A. J. Heeger, *Science*, 1995, **270**, 1789–1791.
3 G. Li, V. Shrotriya, Y. Yao and Y. Yang, *J. Appl. Phys.*, 2005, **98**, 043704–043708.
4 K. M. Coakley and M. D. McGehee, *Chem. Mater.*, 2004, **16**, 4533–4542.
5 P. Peumans, V. Bulovic and S. R. Forrest, *Appl. Phys. Lett.*, 2000, **76**, 2650–2652.
6 J. Liu, M. A. G. Namboothiry and D. L. Carroll, *Appl. Phys. Lett.*, 2007, **90**, 133515–133517.
7 B. O'Connor, D. Nothern, K. P. Pipe and M. Shtein, *Opt. Express*, 2010, **18**, A432–A443.
8 M. Niggemann, M. Glatthaar, P. Lewer, C. Müller, J. Wagner and A. Gombert, *Thin Solid Films*, 2006, **511–512**, 628–633.
9 S.-B. Rim, S. Zhao, S. R. Scully, M. D. McGehee and P. Peumans, *Appl. Phys. Lett.*, 2007, **91**, 243501–243503.
10 K. Tvingstedt, V. Andersson, F. Zhang and O. Inganäs, *Appl. Phys. Lett.*, 2007, **91**, 123514–123516.
11 K. Tvingstedt, S. Dal Zilio, O. Inganäs and M. Tormen, *Opt. Express*, 2008, **16**, 21608–21615.
12 S. D. Zilio, K. Tvingstedt, O. Inganäs and M. Tormen, *Microelectron. Eng.*, 2009, **86**, 1150–1154.
13 E. Yablonovitch, *J. Opt. Soc. Am.*, 1982, **72**, 899–907.
14 P. Campbell and M. A. Green, *IEEE Trans. Electron Devices*, 1986, **33**, 234–239.
15 Z. Yu, A. Raman and S. Fan, *Proc. Natl. Acad. Sci. U. S. A.*, 2010, **107**, 17491–17496.
16 Z. Yu, A. Raman and S. Fan, *Opt. Express*, 2010, **18**, A366–A380.
17 D. Duche, L. Escoubas, J.-J. Simon, P. Torchio, W. Vervisch and F. Flory, *Appl. Phys. Lett.*, 2008, **92**, 193310–193312.

18 J. R. Tumbleston, D.-H. Ko, E. T. Samulski and R. Lopez, *Appl. Phys. Lett.*, 2009, **94**, 043305–043307.
19 J. G. Mutitu, S. Shi, C. Chen, T. Creazzo, A. Barnett, C. Honsberg and D. W. Prather, *Opt. Express*, 2008, **16**, 15238–15248.
20 P. Bermel, C. Luo, L. Zeng, L. C. Kimerling and J. D. Joannopoulos, *Opt. Express*, 2007, **15**, 16986–17000.
21 Y. Park, E. Drouard, O. El Daif, X. Letartre, P. Viktorovitch, A. Fave, A. Kaminski, M. Lemiti and C. Seassal, *Opt. Express*, 2009, **17**, 14312–14321.
22 L. Zeng, Y. Yi, C. Hong, J. Liu, N. Feng, X. Duan, L. C. Kimerling and B. A. Alamariu, *Appl. Phys. Lett.*, 2006, **89**, 111111–111113.
23 D.-H. Ko, J. R. Tumbleston, L. Zhang, S. Williams, J. M. DeSimone, R. Lopez and E. T. Samulski, *Nano Lett.*, 2009, **9**, 2742–2746.
24 D.-H. Ko, J. R. Tumbleston, W. Schenck, R. Lopez and E. T. Samulski, *J. Phys. Chem. C*, 2011, **115**, 4247–4254.
25 S. Guldin, S. Huttner, M. Kolle, M. E. Welland, P. Muller-Buschbaum, R. H. Friend, U. Steiner and N. Tetreault, *Nano Lett.*, 2010, **10**, 2303–2309.
26 S. Nishimura, N. Abrams, B. A. Lewis, L. I. Halaoui, T. E. Mallouk, K. D. Benkstein, J. van de Lagemaat and A. J. Frank, *J. Am. Chem. Soc.*, 2003, **125**, 6306–6310.
27 S. Colodrero, A. Mihi, L. Häggman, M. Ocaña, G. Boschloo, A. Hagfeldt and H. Míguez, *Adv. Mater.*, 2009, **21**, 764–770.
28 I. Rodriguez, F. Ramiro-Manzano, P. Atienzar, J. M. Martinez, F. Meseguer, H. Garcia and A. Corma, *J. Mater. Chem.*, 2007, **17**, 3205–3209.
29 E. T. Yu, J. v. d and Lagemaat, *MRS Bull.*, 2011, **36**, 424–428.
30 A. J. Morfa, K. L. Rowlen, T. H. Reilly, Iii, M. J. Romero and J. van de Lagemaat, *Appl. Phys. Lett.*, 2008, **92**, 013504–013506.
31 J.-L. Wu, F.-C. Chen, Y.-S. Hsiao, F.-C. Chien, P. Chen, C.-H. Kuo, M. H. Huang and C.-S. Hsu, *ACS Nano*, 2011, **5**, 959–967.
32 M.-G. Kang, T. Xu, H. J. Park, X. Luo and L. J. Guo, *Adv. Mater.*, 2010, **22**, 4378–4383.
33 S.-S. Kim, S.-I. Na, J. Jo, D.-Y. Kim and Y.-C. Nah, *Appl. Phys. Lett.*, 2008, **93**, 073307–073309.
34 N. C. Lindquist, W. A. Luhman, S.-H. Oh and R. J. Holmes, *Appl. Phys. Lett.*, 2008, **93**, 123308–123310.
35 W.-J. Yoon, K.-Y. Jung, J. Liu, T. Duraisamy, R. Revur, F. L. Teixeira, S. Sengupta and P. R. Berger, *Sol. Energy Mater. Sol. Cells*, 2010, **94**, 128–132.
36 C. Min, J. Li, G. Veronis, J.-Y. Lee, S. Fan and P. Peumans, *Appl. Phys. Lett.*, 2010, **96**, 133302–133304.
37 M. A. Sefunc, A. K. Okyay and H. V. Demir, *Appl. Phys. Lett.*, 2011, **98**, 093117–093119.
38 T. H. Reilly, Iii, J. van de Lagemaat, R. C. Tenent, A. J. Morfa and K. L. Rowlen, *Appl. Phys. Lett.*, 2008, **92**, 243304–243306.
39 J. K. Mapel, M. Singh, M. A. Baldo and K. Celebi, *Appl. Phys. Lett.*, 2007, **90**, 121102–121104.
40 S. Vedraine, P. Torchio, D. Duché, F. Flory, J.-J. Simon, J. Le Rouzo and L. Escoubas, *Sol. Energy Mater. Sol. Cells*, 2011, **95**, 57–64.
41 B. P. Rand, P. Peumans and S. R. Forrest, *J. Appl. Phys.*, 2004, **96**, 7519–7526.
42 K. Tvingstedt, N.-K. Persson, O. Inganäs, A. Rahachou and I. V. Zozoulenko, *Appl. Phys. Lett.*, 2007, **91**, 113514–113516.
43 S. Pillai and M. A. Green, *Sol. Energy Mater. Sol. Cells*, 2010, **94**, 1481–1486.
44 H. A. Atwater and A. Polman, *Nat. Mater.*, 2010, **9**, 205–213.
45 V. E. Ferry, J. N. Munday and H. A. Atwater, *Adv. Mater.*, 2010, **22**, 4794–4808.
46 F.-C. Chen, J.-L. Wu, C.-L. Lee, Y. Hong, C.-H. Kuo and M. H. Huang, *Appl. Phys. Lett.*, 2009, **95**, 013305–013307.
47 H. Shen, P. Bienstman and B. Maes, *J. Appl. Phys.*, 2009, **106**, 073109–073113.
48 J. Feng, T. Okamoto, R. Naraoka and S. Kawata, *Appl. Phys. Lett.*, 2008, **93**, 051106–051108.
49 A. Abass, H. Shen, P. Bienstman and B. Maes, *J. Appl. Phys.*, 2011, **109**, 023111–023117.
50 M. Niggemann, M. Glatthaar, A. Gombert, A. Hinsch and V. Wittwer, *Thin Solid Films*, 2004, **451–452**, 619–623.
51 D. H. Wang, D.-G. Choi, K.-J. Lee, J.-H. Jeong, S. H. Jeon, O. O. Park and J. H. Park, *Org. Electron.*, 2010, **11**, 285–290.
52 L. S. Roman, O. Inganäs, T. Granlund, T. Nyberg, M. Svensson, M. R. Andersson and J. C. Hummelen, *Adv. Mater.*, 2000, **12**, 189–195.
53 C. Cocoyer, L. Rocha, L. Sicot, B. Geffroy, R. de Bettignies, C. Sentein, C. Fiorini-Debuisschert and P. Raimond, *Appl. Phys. Lett.*, 2006, **88**, 133108–133110.
54 S.-I. Na, S.-S. Kim, J. Jo, S.-H. Oh, J. Kim and D.-Y. Kim, *Adv. Funct. Mater.*, 2008, **18**, 3956–3963.
55 K. S. Nalwa, J.-M. Park, K.-M. Ho and S. Chaudhary, *Adv. Mater.*, 2011, **23**, 112–116.
56 B. G. Prevo, E. W. Hon and O. D. Velev, *J. Mater. Chem.*, 2007, **17**, 791–799.
57 J. Zhu, Z. Yu, G. F. Burkhard, C.-M. Hsu, S. T. Connor, Y. Xu, Q. Wang, M. McGehee, S. Fan and Y. Cui, *Nano Lett.*, 2008, **9**, 279–282.
58 K. Forberich, G. Dennler, M. C. Scharber, K. Hingerl, T. Fromherz and C. J. Brabec, *Thin Solid Films*, 2008, **516**, 7167–7170.
59 W. C. Luk, K. M. Yeung, K. C. Tam, K. L. Ng, K. C. Kwok, C. Y. Kwong, A. M. C. Ng and A. B. Djurišic, *Org. Electron.*, 2011, **12**, 557–561.
60 T. Søndergaard, J. Gadegaard, P. K. Kristensen, T. K. Jensen, T. G. Pedersen and K. Pedersen, *Opt. Express*, 2010, **18**, 26245–26258.
61 S.-J. Choi and S.-Y. Huh, *Macromol. Rapid Commun.*, 2009, **31**, 539–544.
62 S. John, *Phys. Rev. Lett.*, 1987, **58**, 2486.
63 E. Yablonovitch, *Phys. Rev. Lett.*, 1987, **58**, 2059.
64 Y.-J. Lee, S.-H. Kim, J. Huh, G.-H. Kim, Y.-H. Lee, S.-H. Cho, Y.-C. Kim and Y. R. Do, *Appl. Phys. Lett.*, 2003, **82**, 3779–3781.
65 C. Liu, V. Kamaev and Z. V. Vardeny, *Appl. Phys. Lett.*, 2005, **86**, 143501–143503.
66 J. Wang, X. Sun, L. Chen and S. Y. Chou, *Appl. Phys. Lett.*, 1999, **75**, 2767–2769.
67 E. Chow, A. Grot, L. W. Mirkarimi, M. Sigalas and G. Girolami, *Opt. Lett.*, 2004, **29**, 1093–1095.
68 X. Fan, I. M. White, S. I. Shopova, H. Zhu, J. D. Suter and Y. Sun, *Anal. Chim. Acta*, 2008, **620**, 8–26.
69 H. Y. Fu, H. Y. Tam, L.-Y. Shao, X. Dong, P. K. A. Wai, C. Lu and S. K. Khijwania, *Appl. Opt.*, 2008, **47**, 2835–2839.
70 R. Xuan, Q. Wu, Y. Yin and J. Ge, *J. Mater. Chem.*, 2011, **21**, 3672–3676.
71 C. Chen, Y. Zhu, H. Bao, J. Shen, H. Jiang, L. Peng, X. Yang, C. Li and G. Chen, *Chem. Commun.*, 2011, **47**, 5530–5532.
72 A. C. Arsenault, V. Kitaev, I. Manners, G. A. Ozin, A. Mihi and H. Miguez, *J. Mater. Chem.*, 2005, **15**, 133–138.
73 E. Garnett and P. Yang, *Nano Lett.*, 2010, **10**, 1082–1087.
74 Y. Zhang, J. Wang, Y. Zhao, J. Zhai, L. Jiang, Y. Song and D. Zhu, *J. Mater. Chem.*, 2008, **18**, 2650–2652.
75 W. Wiedemann, L. Sims, A. Abdellah, A. Exner, R. Meier, K. P. Musselman, J. L. MacManus-Driscoll, P. Muller-Buschbaum, G. Scarpa, P. Lugli and L. Schmidt-Mende, *Appl. Phys. Lett.*, 2010, **96**, 263109–263111.
76 D. Duché, E. Drouard, J. J. Simon, L. Escoubas, P. Torchio, J. Le Rouzo and S. Vedraine, *Sol. Energy Mater. Sol. Cells*, 2011, **95**, 18–25.
77 J. R. Tumbleston, D.-H. Ko, E. T. Samulski and R. Lopez, *Opt. Express*, 2009, **17**, 7670–7681.
78 M. Agrawal and P. Peumans, *Opt. Express*, 2008, **16**, 5385–5396.
79 B. Park, M. Kim and Y. Lee, *Sol. Energy Mater. Sol. Cells*, 2011, **95**, 1141–1145.
80 Y. Doi, A. Saeki, Y. Koizumi, S. Seki, K. Okamoto, T. Kozawa and S. Tagawa, *J. Vac. Sci. Technol., B*, 2005, **23**, 2051–2055.
81 S.-I. Na, S.-S. Kim, S.-S. Kwon, J. Jo, J. Kim, T. Lee and D.-Y. Kim, *Appl. Phys. Lett.*, 2007, **91**, 173509–173511.
82 J. P. Rolland, B. W. Maynor, L. E. Euliss, A. E. Exner, G. M. Denison and J. M. DeSimone, *J. Am. Chem. Soc.*, 2005, **127**, 10096–10100.
83 J. P. Rolland, E. C. Hagberg, G. M. Denison, K. R. Carter and J. M. De Simone, *Angew. Chem., Int. Ed.*, 2004, **43**, 5796–5799.
84 M. Aryal, K. Trivedi and W. Hu, *ACS Nano*, 2009, **3**, 3085–3090.
85 M.-S. Kim, J.-S. Kim, J. C. Cho, M. Shtein, L. J. Guo and J. Kim, *Appl. Phys. Lett.*, 2007, **90**, 123113–123115.
86 X. He, F. Gao, G. Tu, D. Hasko, S. HuÎttner, U. Steiner, N. C. Greenham, R. H. Friend and W. T. S. Huck, *Nano Lett.*, 2010, **10**, 1302–1307.
87 D. Cheyns, K. Vasseur, C. Rolin, J. Genoe, J. Poortmans and P. Heremans, *Nanotechnology*, 2008, **19**, 424016.


 

88 Z. Zheng, K.-H. Yim, M. S. M. Saifullah, M. E. Welland, R. H. Friend, J.-S. Kim and W. T. S. Huck, *Nano Lett.*, 2007, **7**, 987–992.
89 Z. Hu, B. t. Muls, L. k. Gence, D. A. Serban, J. Hofkens, S. Melinte, B. Nysten, S. Demoustier-Champagne and A. M. Jonas, *Nano Lett.*, 2007, **7**, 3639–3644.
90 J. S. Kim, Y. Park, D. Y. Lee, J. H. Lee, J. H. Park, J. K. Kim and K. Cho, *Adv. Funct. Mater.*, 2010, **20**, 540–545.
91 K. M. Coakley, B. S. Srinivasan, J. M. Ziebarth, C. Goh, Y. Liu and M. D. McGehee, *Adv. Funct. Mater.*, 2005, **15**, 1927–1932.
92 N. Haberkorn, J. S. Gutmann and P. Theato, *ACS Nano*, 2009, **3**, 1415–1422.
93 J. W. Lee, K. Kim, D. H. Park, M. Y. Cho, Y. B. Lee, J. S. Jung, D.-C. Kim, J. Kim and J. Joo, *Adv. Funct. Mater.*, 2009, **19**, 704–710.
94 M. Aryal, F. Buyukserin, K. Mielczarek, X.-M. Zhao, J. Gao, A. Zakhidov and W. Hu, *J. Vac. Sci. Technol., B: Microelectron. Nanometer Struct.–Process., Meas., Phenom.*, 2008, **26**, 2562–2566.
95 D. O'Carroll, I. Lieberwirth and G. Redmond, *Nat. Nanotechnol.*, 2007, **2**, 180–184.
96 R. C. Furneaux, W. R. Rigby and A. P. Davidson, *Nature*, 1989, **337**, 147–149.
97 C. Goh, K. M. Coakley and M. D. McGehee, *Nano Lett.*, 2005, **5**, 1545–1549.
98 S. Baek, J. B. Park, W. Lee, S.-H. Han, J. Lee and S.-H. Lee, *New J. Chem.*, 2009, **33**, 986–990.
99 C. A. Foss, M. J. Tierney and C. R. Martin, *J. Phys. Chem.*, 1992, **96**, 9001–9007.
100 C. R. Martin, *Science*, 1994, **266**, 1961–1966.
101 M. Zhou, M. Aryal, K. Mielczarek, A. Zakhidov and W. Hu, *J. Vac. Sci. Technol., B: Microelectron. Nanometer Struct.–Process., Meas., Phenom.*, 2010, **28**, C6M63–C66M67.
102 Y. Yang, M. Aryal, K. Mielczarek, W. Hu and A. Zakhidov, *J. Vac. Sci. Technol., B: Microelectron. Nanometer Struct.–Process., Meas., Phenom.*, 2010, **28**, C6M104–C106M107.
103 C. F. Shih, K. T. Hung, J. W. Wu, C. Y. Hsiao and W. M. Li, *Appl. Phys. Lett.*, 2009, **94**, 143505–143507.
104 S. S. Williams, S. Retterer, R. Lopez, R. Ruiz, E. T. Samulski and J. M. DeSimone, *Nano Lett.*, 2010, **10**, 1421–1428.
105 B. D. Gates and G. M. Whitesides, *J. Am. Chem. Soc.*, 2003, **125**, 14986–14987.
106 L. Stolz Roman, O. Inganäs, T. Granlund, T. Nyberg, M. Svensson, M. R. Andersson and J. C. Hummelen, *Adv. Mater.*, 2000, **12**, 189–195.
107 F. Zhang, T. Nyberg and O. Inganäs, *Nano Lett.*, 2002, **2**, 1373–1377.
108 M. Gaal, C. Gadermaier, H. Plank, E. Moderegger, A. Pogantsch, G. Leising and E. J. W. List, *Adv. Mater.*, 2003, **15**, 1165–1167.
109 B. K. Mandal, R. J. Jeng, J. Kumar and S. K. Tripathy, *Makromol. Chem. Rapid Commun.*, 1991, **12**, 607–612.
110 S.-S. Kim, C. Chun, J.-C. Hong and D.-Y. Kim, *J. Mater. Chem.*, 2006, **16**, 370–375.
111 A. Bietsch and B. Michel, *J. Appl. Phys.*, 2000, **88**, 4310–4318.
112 J. N. Lee, C. Park and G. M. Whitesides, *Anal. Chem.*, 2003, **75**, 6544–6554.
113 T. T. Truong, R. Lin, S. Jeon, H. H. Lee, J. Maria, A. Gaur, F. Hua, I. Meinel and J. A. Rogers, *Langmuir*, 2007, **23**, 2898–2905.
114 S. E. A. Gratton, S. S. Williams, M. E. Napier, P. D. Pohlhaus, Z. Zhou, K. B. Wiles, B. W. Maynor, C. Shen, T. Olafsen, E. T. Samulski and J. M. DeSimone, *Acc. Chem. Res.*, 2008, **41**, 1685–1695.
115 R. Riehn, A. Charas, J. Morgado and F. Cacialli, *Appl. Phys. Lett.*, 2003, **82**, 526–528.
116 F. Cacialli, R. Riehn, A. Downes, G. Latini, A. Charas and J. Morgado, *Ultramicroscopy*, 2004, **100**, 449–455.
117 D. Credgington, O. Fenwick, A. Charas, J. Morgado, K. Suhling and F. Cacialli, *Adv. Funct. Mater.*, 2010, **20**, 2842–2847.
118 A. Charas, H. Alves, J. M. G. Martinho, L. Alcácer, O. Fenwick, F. Cacialli and J. Morgado, *Synth. Met.*, 2008, **158**, 643–653.
119 R. Robert and C. Franco, *J. Opt. A: Pure Appl. Opt.*, 2005, **7**, S207–S212.
120 N. S. Losilla, J. Martinez, E. Bystrenova, P. Greco, F. Biscarini and R. García, *Ultramicroscopy*, 2010, **110**, 729–732.
121 O. Fenwick, L. Bozec, D. Credgington, A. Hammiche, G. M. Lazzerini, Y. R. Silberberg and F. Cacialli, *Nat. Nanotechnol.*, 2009, **4**, 664–668.
122 J. H. Lim and C. A. Mirkin, *Adv. Mater.*, 2002, **14**, 1474–1477.
123 D. C. Coffey and D. S. Ginger, *J. Am. Chem. Soc.*, 2005, **127**, 4564–4565.
124 L. Y. Park, A. M. Munro and D. S. Ginger, *J. Am. Chem. Soc.*, 2008, **130**, 15916–15926.
125 A. Noy, A. E. Miller, J. E. Klare, B. L. Weeks, B. W. Woods and J. J. DeYoreo, *Nano Lett.*, 2001, **2**, 109–112.
126 S. H. M. Persson, P. Dyreklev and O. Inganäs, *Adv. Mater.*, 1996, **8**, 405–408.
127 R. Stabile, A. Camposeo, L. Persano, S. Tavazzi, R. Cingolani and D. Pisignano, *Appl. Phys. Lett.*, 2007, **91**, 101110–101112.
128 B. W. Maynor, S. F. Filocamo, M. W. Grinstaff and J. Liu, *J. Am. Chem. Soc.*, 2001, **124**, 522–523.
129 H. J. Levinson, M. A. McCord, F. Cerrina, R. D. Allen, J. G. Skinner, A. R. Neureuther, M. C. Peckerar, F. K. Perkins and Michael J. Rooks, *Handbook of Microlithography, Micromachining and Microfabrication* Society of Photo-Optical Instrumentation Engineers, Bellingham, WA, 1997.
130 J. I. Lee, S. H. Cho, S.-M. Park, J. K. Kim, J. K. Kim, J.-W. Yu, Y. C. Kim and T. P. Russell, *Nano Lett.*, 2008, **8**, 2315–2320.
131 E. J. W. Crossland, M. Kamperman, M. Nedelcu, C. Ducati, U. Wiesner, D. M. Smilgies, G. E. S. Toombes, M. A. Hillmyer, S. Ludwigs, U. Steiner and H. J. Snaith, *Nano Lett.*, 2008, **9**, 2807–2812.
132 E. J. W. Crossland, M. Nedelcu, C. Ducati, S. Ludwigs, M. A. Hillmyer, U. Steiner and H. J. Snaith, *Nano Lett.*, 2008, **9**, 2813–2819.
133 A. Vlad, C. A. Dutu, P. Guillet, P. Jedrasik, C.-A. Fustin, U. Sodervall, J.-F. Gohy and S. Melinte, *Nano Lett.*, 2009, **9**, 2838–2843.
134 H.-Y. Chen, J. Hou, S. Zhang, Y. Liang, G. Yang, Y. Yang, L. Yu, Y. Wu and G. Li, *Nat. Photonics*, 2009, **3**, 649–653.